ELECTRIC POWER RESEARCH INSTITUTE

Welding and Repair Technology Center: Instantaneous Power Monitoring for Gas Metal Arc Welding Process

1022881

Welding and Repair Technology Center: Instantaneous Power Monitoring for Gas Metal Arc Welding Process

1022881

Technical Update, October 2011

EPRI Project Manager

G. Frederick

This document does **NOT** meet the requirements of
10CFR50 Appendix B, 10CFR Part 21,
ANSI N45.2-1977 and/or the intent of ISO-9001 (1994)

ELECTRIC POWER RESEARCH INSTITUTE
3420 Hillview Avenue, Palo Alto, California 94304-1338 ▪ PO Box 10412, Palo Alto, California 94303-0813 ▪ USA
800.313.3774 ▪ 650.855.2121 ▪ askepri@epri.com ▪ www.epri.com

DISCLAIMER OF WARRANTIES AND LIMITATION OF LIABILITIES

THIS DOCUMENT WAS PREPARED BY THE ORGANIZATION(S) NAMED BELOW AS AN ACCOUNT OF WORK SPONSORED OR COSPONSORED BY THE ELECTRIC POWER RESEARCH INSTITUTE, INC. (EPRI). NEITHER EPRI, ANY MEMBER OF EPRI, ANY COSPONSOR, THE ORGANIZATION(S) BELOW, NOR ANY PERSON ACTING ON BEHALF OF ANY OF THEM:

(A) MAKES ANY WARRANTY OR REPRESENTATION WHATSOEVER, EXPRESS OR IMPLIED, (I) WITH RESPECT TO THE USE OF ANY INFORMATION, APPARATUS, METHOD, PROCESS, OR SIMILAR ITEM DISCLOSED IN THIS DOCUMENT, INCLUDING MERCHANTABILITY AND FITNESS FOR A PARTICULAR PURPOSE, OR (II) THAT SUCH USE DOES NOT INFRINGE ON OR INTERFERE WITH PRIVATELY OWNED RIGHTS, INCLUDING ANY PARTY'S INTELLECTUAL PROPERTY, OR (III) THAT THIS DOCUMENT IS SUITABLE TO ANY PARTICULAR USER'S CIRCUMSTANCE; OR

(B) ASSUMES RESPONSIBILITY FOR ANY DAMAGES OR OTHER LIABILITY WHATSOEVER (INCLUDING ANY CONSEQUENTIAL DAMAGES, EVEN IF EPRI OR ANY EPRI REPRESENTATIVE HAS BEEN ADVISED OF THE POSSIBILITY OF SUCH DAMAGES) RESULTING FROM YOUR SELECTION OR USE OF THIS DOCUMENT OR ANY INFORMATION, APPARATUS, METHOD, PROCESS, OR SIMILAR ITEM DISCLOSED IN THIS DOCUMENT.

REFERENCE HEREIN TO ANY SPECIFIC COMMERCIAL PRODUCT, PROCESS, OR SERVICE BY ITS TRADE NAME, TRADEMARK, MANUFACTURER, OR OTHERWISE, DOES NOT NECESSARILY CONSTITUTE OR IMPLY ITS ENDORSEMENT, RECOMMENDATION, OR FAVORING BY EPRI.

THE FOLLOWING ORGANIZATION(S), UNDER CONTRACT TO EPRI, PREPARED THIS REPORT:

Euroweld

The Ohio State University

Electric Power Research Institute (EPRI)

THE TECHNICAL CONTENTS OF THIS DOCUMENT WERE **NOT** PREPARED IN ACCORDANCE WITH THE EPRI NUCLEAR QUALITY ASSURANCE PROGRAM MANUAL THAT FULFILLS THE REQUIREMENTS OF 10 CFR 50, APPENDIX B AND 10 CFR PART 21, ANSI N45.2-1977 AND/OR THE INTENT OF ISO-9001 (1994). USE OF THE CONTENTS OF THIS DOCUMENT IN NUCLEAR SAFETY OR NUCLEAR QUALITY APPLICATIONS REQUIRES ADDITIONAL ACTIONS BY USER PURSUANT TO THEIR INTERNAL PROCEDURES.

This is an EPRI Technical Update report. A Technical Update report is intended as an informal report of continuing research, a meeting, or a topical study. It is not a final EPRI technical report.

NOTE

For further information about EPRI, call the EPRI Customer Assistance Center at 800.313.3774 or e-mail askepri@epri.com.

ACKNOWLEDGMENTS

The following organization(s), under contract to the Electric Power Research Institute (EPRI), prepared this report:

Euroweld
255 Rolling Hill Rd.
Mooresville, NC 28117

Principal Investigators
W. Newell
L. Moore
B. Gaal

The Ohio State University
Enarson Hall
154 W. 12th Ave.
Columbus, OH 43210

Principal Investigators
B. Elliott
M. Gilloon
S. Seals
N. Ullum

Electric Power Research Institute (EPRI)
1300 West W.T. Harris Blvd.
Charlotte, NC 28262

Principal Investigators
G. Frederick
C. Anderson
D. Shever

This report describes research sponsored by EPRI.

This publication is a corporate document that should be cited in the literature in the following manner:

Welding and Repair Technology Center: Instantaneous Power Monitoring for Gas Metal Arc Welding Process. EPRI, Palo Alto, CA: 2011. 1022881.

ABSTRACT

The specified new method for measuring heat input by using average instantaneous power or energy was amended into the 2010 ASME Boiler and Pressure Vessel (B&PV) Code Section IX, QW-409.1 to accommodate the use of waveform controlled processes. This project evaluates the implementation of ASME QW-409.1(c) for advance waveform gas metal arc welding (GMAW) deposits, through determining the accuracy of various power meters and power supply output (digital displays) as well as determining the consistency of weld deposits between manufacturers using identical welding parameters. Three power sources were selected: Designs A, B, and C. The power supplies were compared with bead-on-plate (BOP) welds on both 304L stainless steel with ER308L wire and on A36 carbon steel with ER70S-6 wire. Wire diameters of 0.035 in. (0.889 mm) and 0.045 in. (1.1430 mm) solid wire were used on each base material to produce four different material/filler combinations for comparison.

Initial results with two of the three power supplies tested has shown that the power source display (digital readout) and the external monitoring (Fluke meter and data acquisition to a lower limit of 7 kHz) were similar for each weld condition. In addition, the welds made with each power source and identical weld parameters (travel speed and wire feed speed) had similar cross-sectional weld geometry. Current test results led to the consensus that the ASME code should include a minimum sampling rate in order to obtain accurate average instantaneous power or energy measurements for advance waveform power supplies.

Keywords

Advance waveform
Gas metal arc welding (GMAW)
Heat input
Instantaneous power

CONTENTS

LIST OF FIGURES

LIST OF TABLES

1
INTRODUCTION/BACKGROUND

The advancement of welding power supply technology has enabled higher precision, accuracy, and overall customization of welding processes. Power sources are now capable of responding very rapidly to the arc conditions, using proper programming of the power source computer and a recent innovation called “waveform shape control technology.” This is especially useful in Gas Metal Arc Welding (GMAW) as it makes the process easier to learn while generating a higher productivity than power supplies from previous generations. However, these recent advancements also require new methods of measuring the heat input, due to the fact that the standard voltmeters and ammeters are not capable of accurately measuring the arc energy. Thus, a new method of calculating the average instantaneous power with external power meters or power supply display panels has been established and updated into the ASME QW409.1 codes. This investigation involves determining the consistency of power meters and power supply displays to assure accurate measurements when using these new advance waveform power supplies for GMAW. Further investigation includes verification that weld deposits made with different power supplies can be duplicated according to the established program settings used by various power supply manufacturers for specific base materials, shielding gas, wire diameters, and filler materials.

The instantaneous power for this process is the determination of power by using the product of current and voltage measurements made at rapid intervals which capture brief changes in the welding waveform. The only way to measure arc energy with waveform control of the power source is to integrate instantaneous voltage and amperage measurements over time. The computer controlled power supplies measure and record the voltage and amperage at the same frequency of the computer controlling the voltage and amperage. The instantaneous arc energy can then be calculated.

The heat input for waveform controlled power sources while operating in non-waveform controlled mode can be calculated using Equation 1.

$$\boldsymbol{Heat\ Input}\left[\frac{\boldsymbol{J}}{\boldsymbol{in}}\left(\frac{\boldsymbol{J}}{\boldsymbol{mm}}\right)\right]=\frac{\boldsymbol{Voltage}\ [\boldsymbol{V}]\times\boldsymbol{Amperage}\ [\boldsymbol{A}]\times\boldsymbol{60}}{\boldsymbol{Travel\ Speed}\left[{}^{\boldsymbol{in}}/_{\boldsymbol{min}}\ \left({}^{\boldsymbol{mm}}/_{\boldsymbol{min}}\right)\right]}$$

Equation 1-1
Heat Input per length (Non-Waveform Controlled)

The following two equations are the new heat input equations effective for waveform and non-waveform controlled welding. Equation 2 is the heat input per length formula for instantaneous energy measurements in joules (J).

$$\boldsymbol{Heat\ Input}\ \left[\frac{\boldsymbol{J}}{\boldsymbol{in}}\left(\frac{\boldsymbol{J}}{\boldsymbol{mm}}\right)\right] = \frac{\boldsymbol{Energy}\ [\boldsymbol{J}]}{\boldsymbol{Weld\ Bead\ Length}\ [\boldsymbol{in}\ (\boldsymbol{mm})]}$$

Equation 1-2
Heat Input per Length using Instantaneous Energy

The equation for heat input per length using instantaneous power measurements in joules per second (J/s) or Watts (W) is:

$$\boldsymbol{Heat\ Input}\ \left[\frac{\boldsymbol{J}}{\boldsymbol{in}}\left(\frac{\boldsymbol{J}}{\boldsymbol{mm}}\right)\right] = \frac{\boldsymbol{Power}\ \left[\boldsymbol{W}\ \left({}^{\boldsymbol{J}}/_{\boldsymbol{s}}\right)\right] \times \boldsymbol{Arc\ Time}\ [\boldsymbol{s}]}{\boldsymbol{Weld\ Bead\ Length}\ [\boldsymbol{in}\ (\boldsymbol{mm})]}$$

Equation 1-3
Heat Input per length using Instantaneous Power

As the heat input increases, the impact strength increases and the yield strength decreases. It is important to understand this relationship in order to produce welds of the desired strength characteristics through proper heat input application. The heat input increase can also be determined by the volume of weld metal measured by either an increase in bead size (width x thickness) or a decrease in length of the weld bead per unit length of electrode. Variation of heat input can greatly affect the weld bead area and properties. Proper heat input is crucial in order to promote a weld metal cooling rate that will successfully develop a weld bead of the desired size and acceptable mechanical properties. Once the voltage range is specified, the heat input can then be adjusted by increasing or decreasing the travel speed.

The weld bead area and weld metal cooling rate have an important role in determining the metal mechanical properties and final microstructure. The weld bead area is inversely related to the yield strength in high strength multi-pass welds. A linear relationship is found between yield strength and the inverse of the cooling rate. The weld bead area and weld metal cooling rate are dependent on the current and travel speed while remaining independent of the arc voltage.

The variation of heat input amongst the different GMAW power supply manufacturers has been evident in the past. New methods of calculating the heat input more accurately on an instantaneous level through advanced waveform controlled power supplies provide a higher consistency of heat input measurements amongst different manufacturers. This investigation will to determine exactly how consistent these power meters and power supply displays are between various manufacturers.

2
PROJECT OBJECTIVES

New possibilities have arisen for power source designers because the voltages and amperages can be sensed by waveform shape controlled power supplies at much greater sampling frequencies. Waveform controlled welding is a welding process modification of the voltage and current wave shape to control characteristics such as droplet shape, penetration, wetting, bead shape, arc energy and transfer mode. There is not a general pulse waveform that can be considered optimal for all GMAW pulse applications, but it can be customized to best fit the desired characteristics of the application. These characteristics can be controlled with high precision because of the ability to rapidly control voltage and amperage. The elevated precision allows for greater control of metal transfer across the arc in pulse spray welding, which will be observed on a high speed camera for a comparative analysis. Compare welds made by three different advance waveform power sources, with the same heat inputs, by analyzing the weld dilution, weld bead geometry and heat affected zone.

The accuracy of various power supply displays and power meters will be evaluated as they record energy output from various power supplies. This is done using ER308L and E70S-6 solid wires with 0.035-inch and 0.045-inch wire diameter, on 304L stainless steel and mild carbon steel base materials in the flat welding position. Optimal GMAW welding parameters will be applied and recorded for use in the study. As the energy output is recorded, additional weld samples will be manufactured at the identical energy level in terms of joules per inch. A direct comparison will be made, while holding all conditions constant, to determine if consistent weld deposits are being made between the different power supplies. The bead geometry, dilution, voltage, amperage, travel speed, wire feed speed and arc characteristics will all be documented for further analysis.

The scope will include:

- Utilize high speed photography to assure welding power sources have optimized welding parameters for desired material, wire diameters, and deposition rates.
- Measure heat inputs using several different data acquisition rates to determine the instantaneous power measurement and compare their effectiveness related to the power supply digital output.
- Show the importance of sampling frequency through manipulation of the data. Determine the minimum frequency of data acquisition.
- Measure bead profile of weld cross section, to metallographically verify heat input and weld dilution consistency between power supplies.

3
EXPERIMENTAL PROCEDURE

3.1 Welding Process and Setup

Three power sources were used, and are referred to as Design A, B and C. Power measurements during welding were taken from a Fluke 345 meter, a 7.5 kHz data acquisition system (DAQ) and the power source digital display. There were four different material/filler combinations that were used. For each material filler combination, bead on plate welds were performed by each power source. The plates used were 0.5-inch thick and circular in shape, so that they could be fit into the chucks of the positioned. The welds were executed using a rotating positioner and a stationary torch as shown in Figure 3-1. An example of sample plate with completed welds is shown in Figure 3-2. A wire feed speed of 250 in/min and travel speed of 15 in/min was used for all welds. Welding deposition was captured using a high-speed camera. A summary of the welding parameters used is provided in Table 3-1. Design C tests have not been completed, and will be included in the next report out.

Figure 3-1
Welding Set-up

Figure 3-2
Finished Welds

Table 3-1
Welding Parameters

Test No.	Machine	Wire Diameter (in.)/Type	Machine Settings		Volts	Amps
			Arc Adj/Util. Arc	Arc Length/ Mode		
1.1	Design A	0.035/ER308L	N/R	0.3	28	120
1.2					28	117
2.1	Design A	0.045/ER308L	N/R	N/R	30	193
2.2					30	201
3.1	Design A	0.045/ER70S-6	4	0.7	23.9	203
3.2					23.9	203
4.1	Design A	0.035/ER70S-6	4	0.8	21.7	128
4.2					21.7	128
5.1	Design B	0.035/ER70S-6	0.5	12	22.1	124
5.2					22.1	124
6.1	Design B	0.045/ER70S-6	1	22	24.6	209
6.2					24.6	214
7.1	Design B	0.045/ER308L	1	44	28.8	180
7.2					28.8	180
8.1	Design B	0.035/ ER308L	2.5	34	27.2	116
8.2					27.2	114

3.2 Weld Bead Profile

All weld samples were cross sectioned and etched to show the weld bead profile. Measurements of the bead profiles were obtained using PAX it software. Bead profile measurements were used to calculate the dilution.

4
RESULTS AND DISCUSSION

4.1 Power Measurements

Table 4-1 contains the average instantaneous power for all of the weld samples as measured by the DAQ, Fluke 385 meter, and power source display. The average instantaneous power from the DAQ was calculated using equation 4. In the third data column of Table 4-1 are the average instantaneous power values for the DAQ with a calibration correction of 0.1541 kJ obtained using linear regression. Percent difference was calculated for each power value versus the corresponding Fluke value using Equation 5. The last column of Table 4-1 contains absolute percent difference for the average Fluke average instantaneous power values between the corresponding welds made by the two designs.

$$\boldsymbol{P_{AIP} = \sum_{i=1}^{n} \frac{I_i \cdot V_i}{n}}$$

Equation 4-1
Average Instantaneous Power

$$\boldsymbol{Percent\ Difference = \frac{A - B}{\left(\frac{A + B}{2}\right)} \times 100\%}$$

Equation 4-2
Percent Difference

Table 4-1
Average Instant Power Measurements

	DAQ (7.0k Hz)	Fluke (15kHz)	Design A	Design B	Percent Difference from Fluke			Absolute Percent Difference (By Design Type)
Sample ID	(kj/s)	(kj/s)	(kj/s)	(kj/s)	DAQ	Design A	Design B	Fluke
Design A SS .035 1-1	3.6	3.6	3.6		0.00%	0.00%		2.82%
Design A SS .035 1-2	3.5	3.6	3.6		2.82%	0.00%		
Design B SS .035 8-1	3.6	3.5		3.5	-2.82%		0.00%	
Design B SS .035 8-2	3.6	3.5		3.5	-2.82%		0.00%	
Design A SS .045 2-1	6.3	6.4	6.2		1.57%	3.17%		8.13%
Design A SS .045 2-2	6.4	6.4	6.2		0.00%	3.17%		
Design B SS .045 7-1	6.0	5.9		5.8	-1.68%		1.71%	
Design B SS .045 7-2	5.9	5.9		5.8	0.00%		1.71%	
Design A CS .045 3-1	5.8	5.9	5.7		1.71%	3.45%		0.00%
Design A CS .045 3-2	5.8	5.9	5.7		1.71%	3.45%		
Design B CS .045 6-1	6.0	5.9		5.8	-1.68%		1.71%	
Design B CS .045 6-2	6.1	5.9		6.0	-3.33%		-1.68%	
Design A CS .035 4-1	3.1	3.2	3.1		3.17%	3.17%		1.55%
Design A CS .035 4-2	3.1	3.2	3.1		3.17%	3.17%		
Design B CS .035 5-1	3.3	3.3		3.3	0.00%			
Design B SS .035 5-2	3.2	3.2		3.2	0.00%			

The Fluke 345 meter had the highest published sampling rate and was recently calibrated to Fluke manufacturing standards; therefore it was chosen to be the standard by which all other values were compared. The Fluke 345 displayed values to the tenth of a kJ. This rounding could have resulted to exaggerated differences of .1 kJ. The highest percent difference for the manufacturers' power displays were 3.45% for design A and 1.71% for design B. Both values are under an arbitrary 5% that could reflect a significant difference. The highest percent difference between the manufacturers' power sources for corresponding weld parameters is 8.13%. This difference could be considered an outlier based upon the resulting metallographic comparison of the welds. The actual parameters (amps and volts) based on the specific power supply optimal settings for this setup (0.045-in., SS, gas mixture) may not be identical to the other power supplies. All other differences between manufactures are under 2.82%.

The voltage, current and power waveforms for mild carbon steel (A36) Design A and B 0.045-in. welding have been plotted and are contained in Figures 4-1 through 4-6. Comparison of these plots shows that waveforms can vary significantly from one power source design to the other. Data points plotted on the graphs were obtained from the DAQ output. This can possibly affect weld bead shape and is discussed in more detail later. A strong illustration of this can be visualized by comparing the voltage plot of Design A with that of Design B. Design B has a much smoother voltage curve while design A has a much choppier voltage curve. It contains a large number of mini voltage peaks.

Differences in the amperage curves between Design B and Design A can be seen quantitatively. Design B has a lower peak amperage than Design A. Conversely, Design B has a higher background amperage that Design A. This shows that two different waveforms can have significantly different shapes but still have the same power output. As discussed later, this has the potential to change the shape of the weld bead. Although most of the weld deposits were similar between the power source designs. in the instance sited here they were not. In future studies it would be advantageous to study this further.

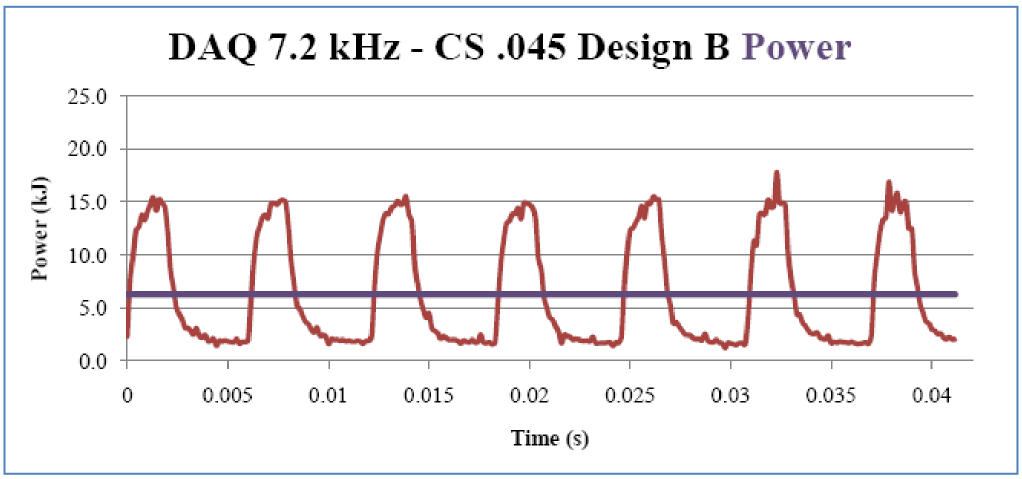

Figure 4-1
DAQ Power Measurement for Design B

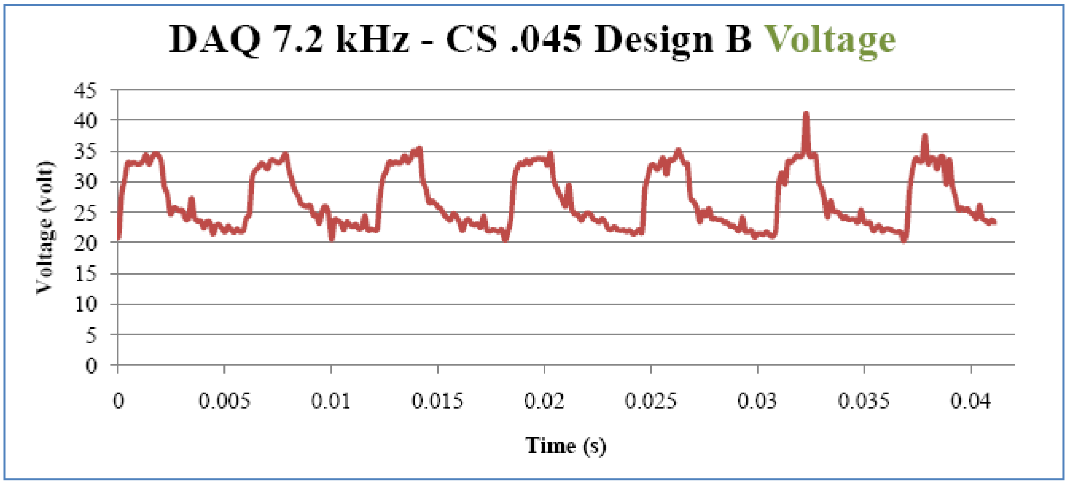

Figure 4-2
DAQ Voltage Measurement for Design B

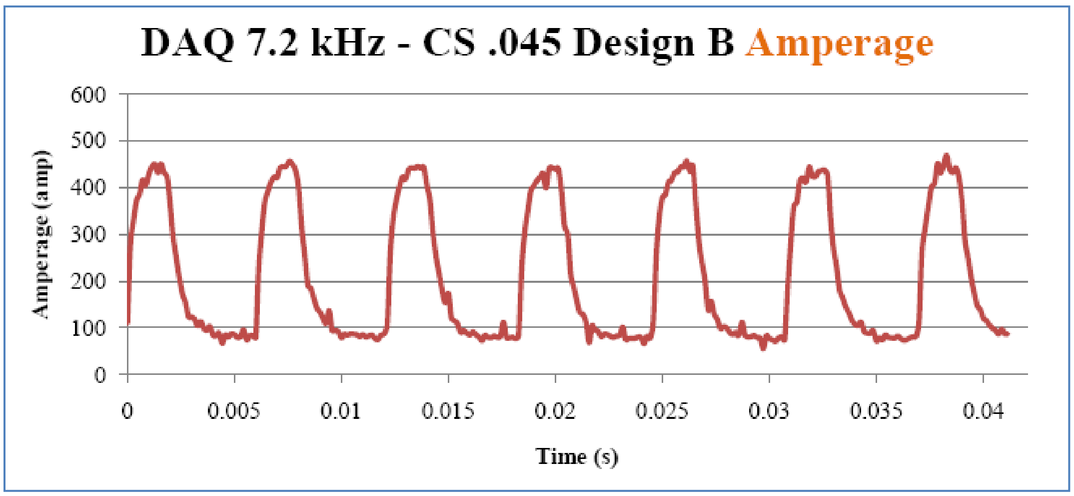

Figure 4-3
DAQ Current Measurement for Design B

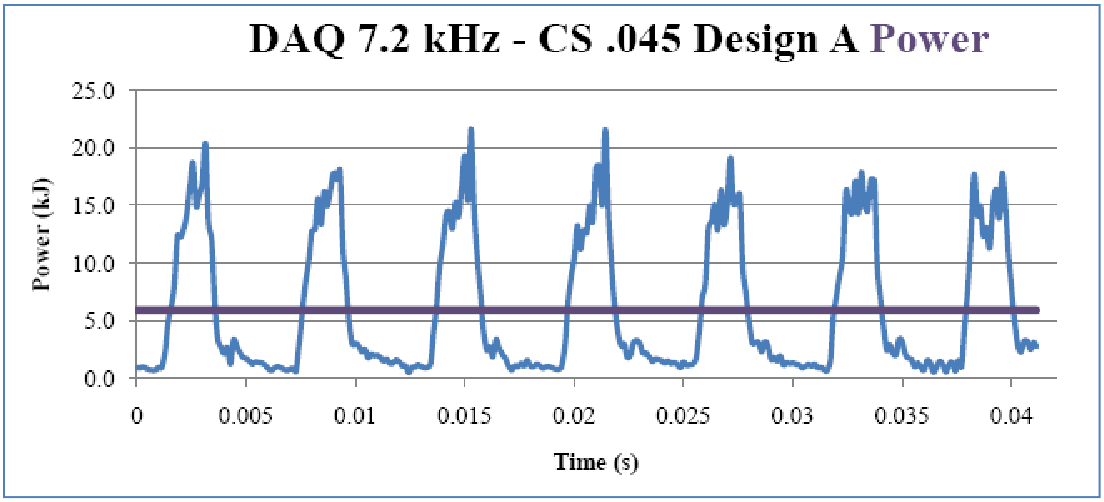

Figure 4-4
DAQ Power Measurement for Design A

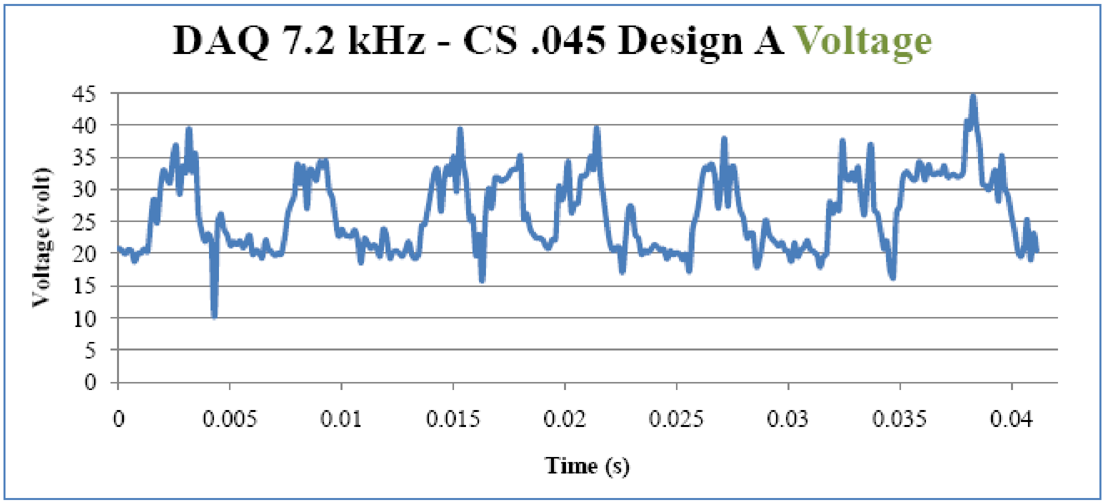

Figure 4-5
DAQ Voltage Measurement for Design A

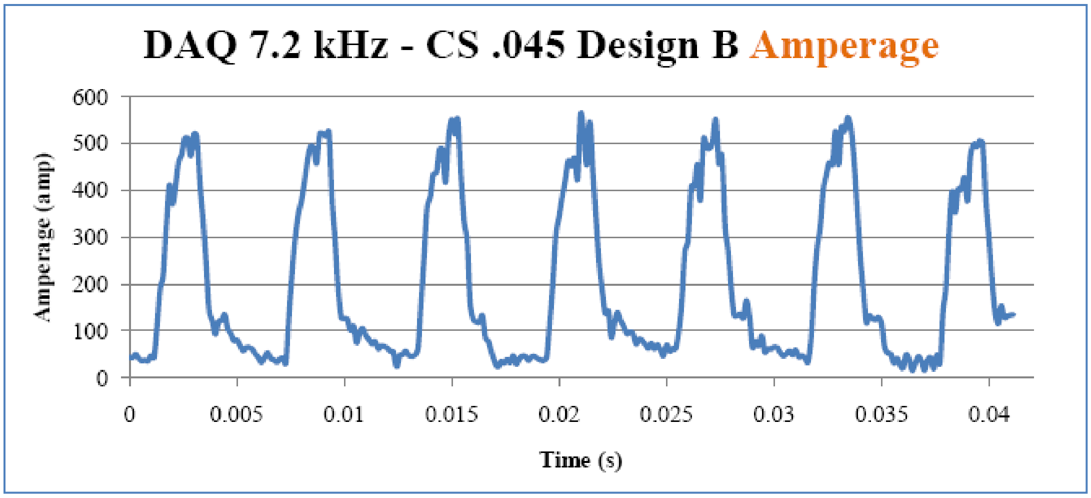

Figure 4-6
DAQ Current Measurement for Design A

Figure 4-7 is a Power Spectrum Density plot of design B's run of .045-in. electrode on mild carfon steel (A 36). The importance of this plot is to show what frequency most of the power is coming from in the complex waveform. The graph is produced by doing a Fourier transform of the power wave. The Fourier transform was done with a Matlab program. For this particular run most of the power is coming from the constant background voltage and current, pulses at 169.4 Hz, and a small faction at 337.9 Hz. Nyquist theorm states that the sampling frequency should be 2x the upper bound frequency components to recreate the waveform. In practice it should be 10x to achieve adequate reconstruction of the waveform. Given that there is no significant power coming from above 337.9 Hz a sampling rate of 3500Hz should be adequate to reproduce this waveform. Matlab data was used to down sample the data obtained from the DAQ at 7 kHz, Figure 10. The resulting data is graphed and presented in Figures 4-9, 4-10, and 4-11 for 3500 Hz, 1750 Hz, and 437 Hz respectively. The 3500 Hz and 1750 Hz show a good reconstruction of the wave form as compared to the 7000 Hz waveform plot. The 437 Hz plot shows a great amount of aliasing and it is not 2x the 337.9 Hz frequency needed to satisfy the Nyquist theorem.

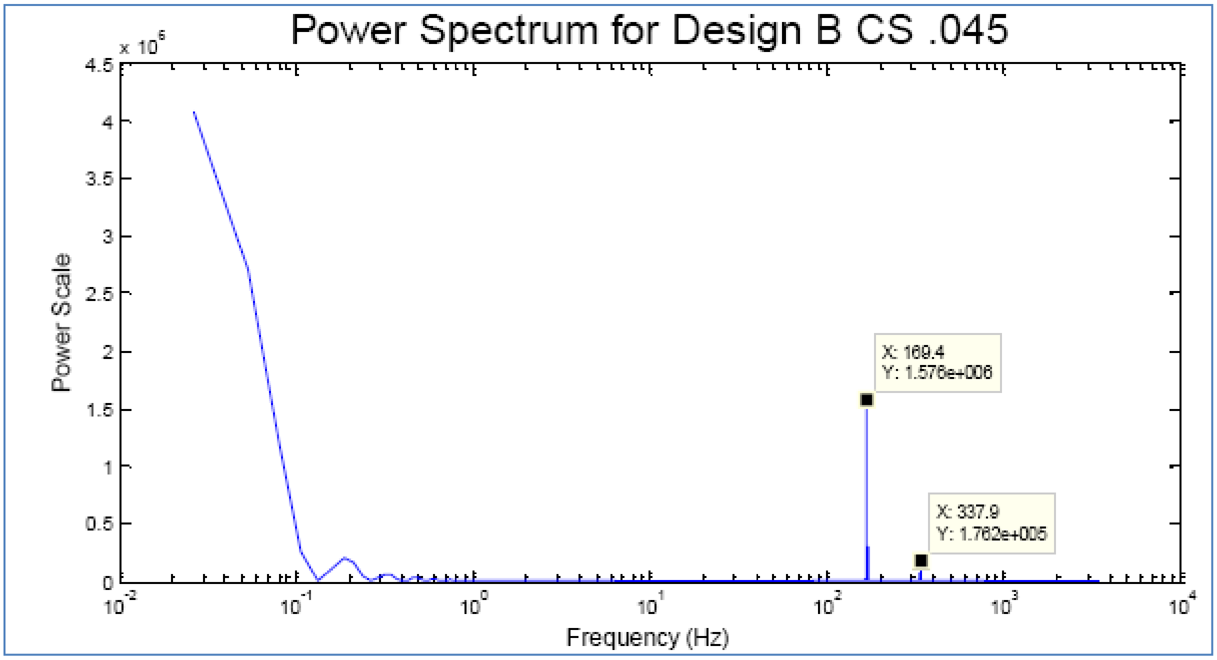

Figure 4-7
Power Spectrum

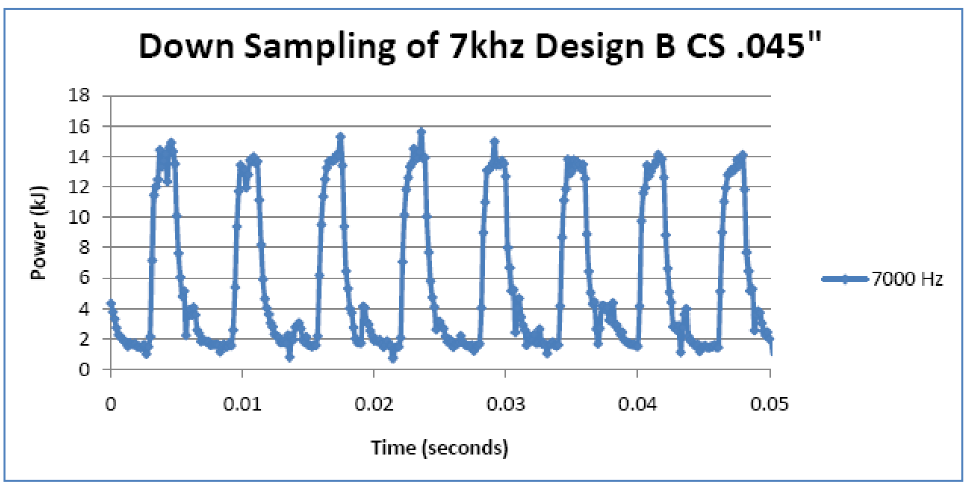

Figure 4-8
Sampling at 7000 Hz.

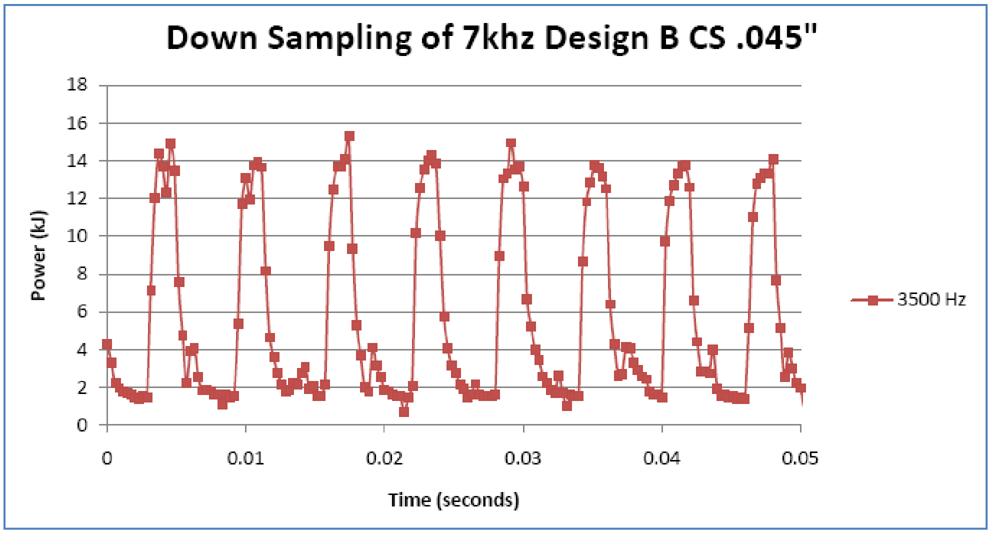

Figure 4-9
Down Sampling 3500 Hz.

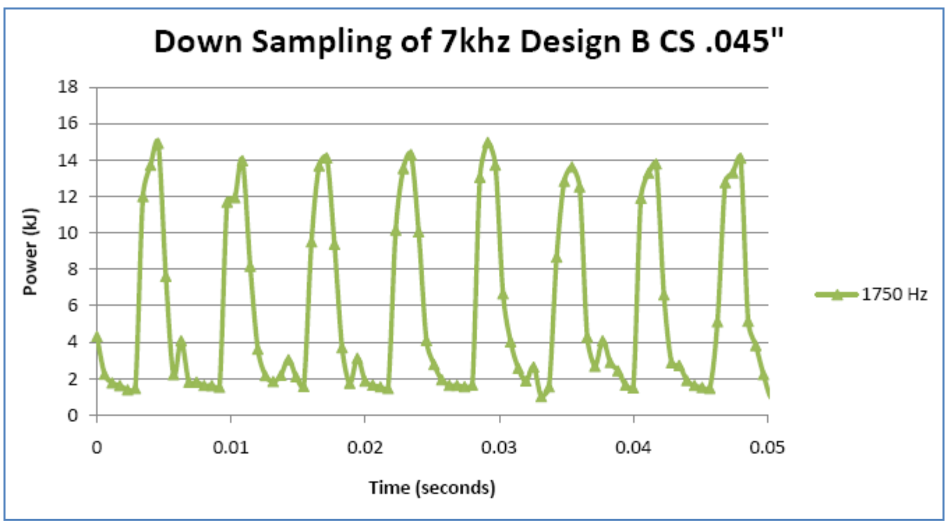

Figure 4-10
Down sampling to 1750 Hz.

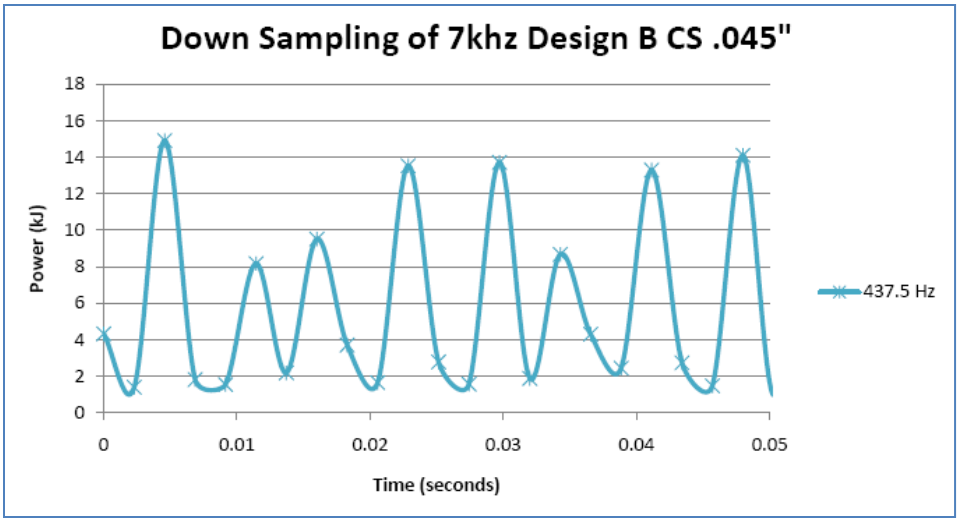

Figure 4-11
Down Sampling to 437.5 Hz.

4.2 Power and Weld bead Profiles

The weld bead dilutions, calculated using the method shown in Figure 4-12, are plotted in Figure 4-13. This plot shows that there was not an appreciable difference between the dilutions from different power source designs when similar heat inputs were used. This is despite significant variations in the waveform shapes, seen above, from one power source design to the other. However, in some instances, the bead shapes varied, despite similar bead areas and dilutions.

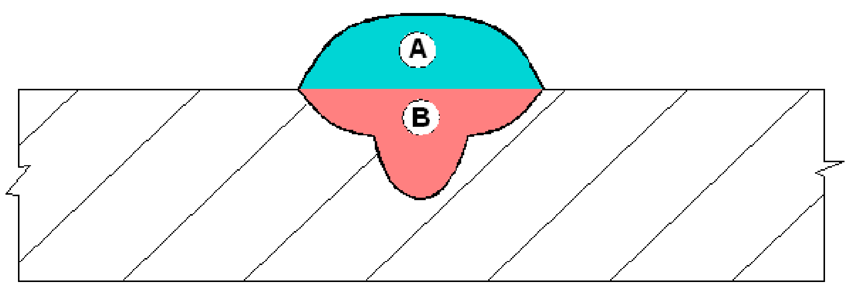

$$\% \, \boldsymbol{Dilution} = \frac{\boldsymbol{B}}{\boldsymbol{A} + \boldsymbol{B}} \times \mathbf{100}$$

Figure 4-12
Standard calculation method for dilution.

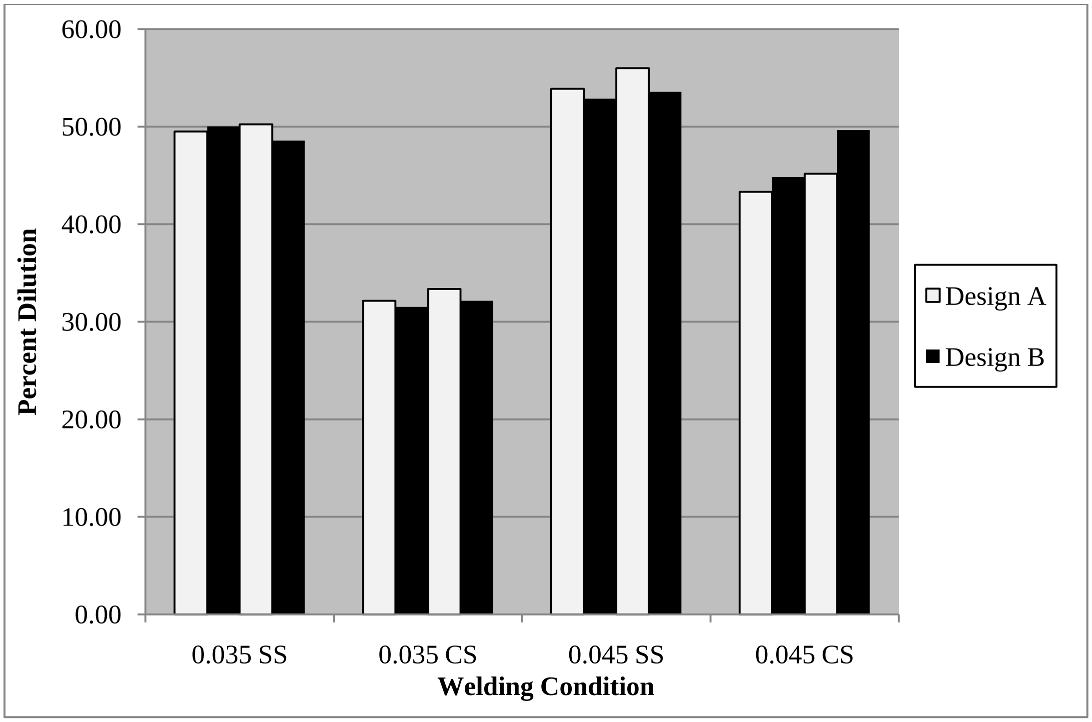

Figure 4-13
Dilution comparison between wire diameters and material type for each power supply design.

Figure 4-17 through 4-20 show a comparison between two bead profiles produced by different power supplies. Some minor discrepancies between the geometry of the weld beads was observed, as seen in Figure 4-17 which was welded using the Design B power source has a wider bead profile with less penetration than the same weld performed using the Design A power source. This was not the case for the other weld samples, which had a similar weld profiles with the different power supply Designs (A,B), Figure 4-18, 4-19 and 4-20. Given the possibility of slight variations in weld bead shape and penetration and thermal profile, it would be prudent for the fabricator to still be cautious, despite similar dilutions, when different welding machines are utilized. Additional metallography is planned to verify consistency in the resulting weld profile. The differences in the pulsed wave forms of the weld machines may lead to changes in bead shape or penetration based on specific attributes utilized to optimize programs for material type, shielding gas, and wire diameter.

Table 4-2
Bead Height, Bead Width and Penetration Measurements

Sample ID	Bead Height	Bead Width	Penetration
	mm	mm	mm
Design A SS .035 1-1	1.99	9.37	2.33
Design A SS .035 1-2	1.78	9.31	2.39
Design B SS .035 8-1	1.76	8.73	2.28
Design B SS .035 8-2	1.84	9.05	2.38
Design A SS .045 2-1	2.67	12.08	3.95
Design A SS .045 2-2	2.5	12.05	3.8
Design B SS .045 7-1	2.55	11.35	4.21
Design B SS .045 7-2	2.41	11.59	4.27
Design A CS .045 3-1	2.93	10.65	3.44
Design A CS .045 3-2	2.69	10.67	3.48
Design B CS .045 6-1	2.77	11.15	3.72
Design B CS .045 6-2	2.45	10.86	3.51
Design A CS .035 4-1	2.31	7.52	1.88
Design A CS .035 4-2	2.25	7.62	1.92
Design B CS .035 5-1	2.17	7.63	1.83
Design B SS .035 5-2	2.19	7.85	1.97

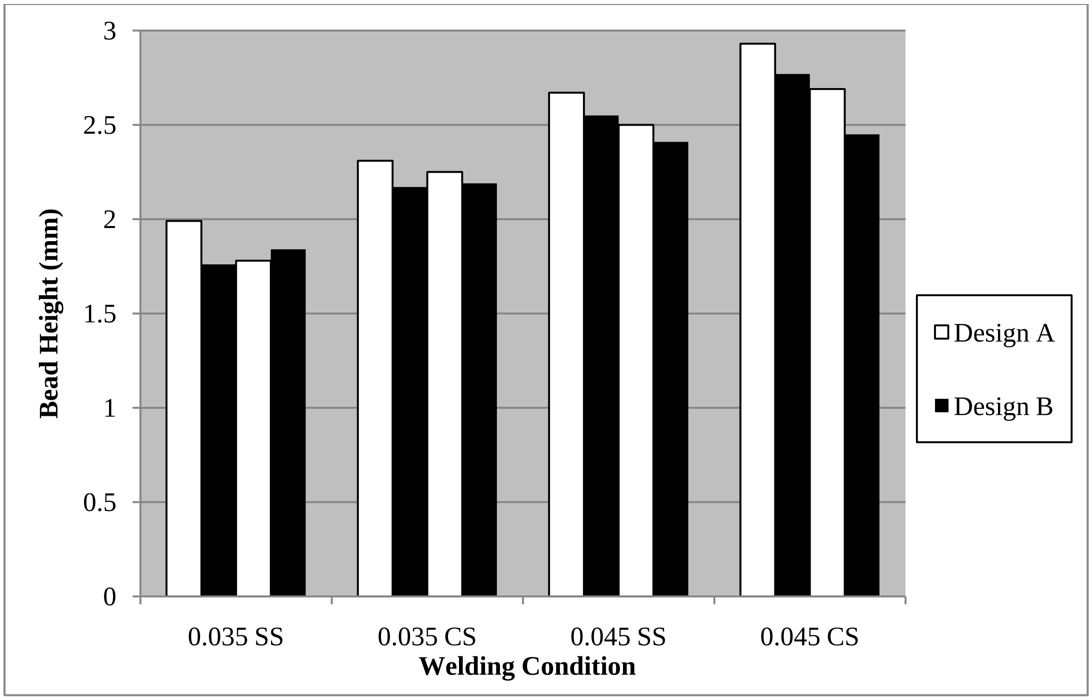

Figure 4-14
Bead height comparison between wire diameters and material type for each power supply design.

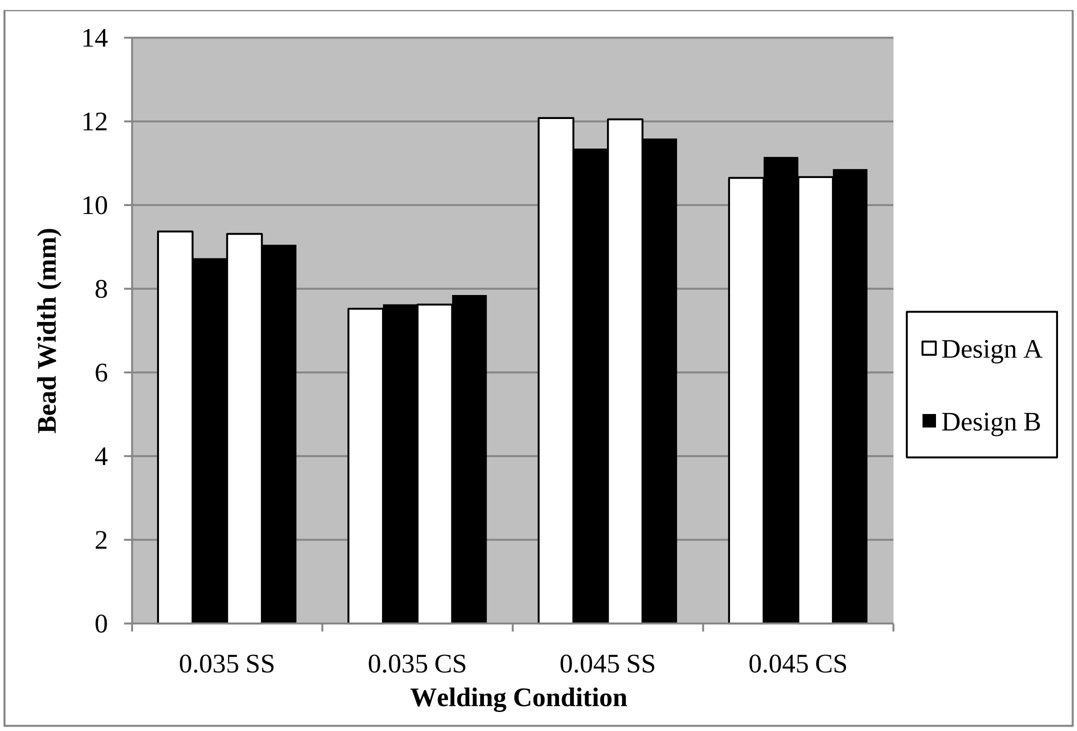

Figure 4-15
Bead width comparison between wire diameters and material type for each power supply design.

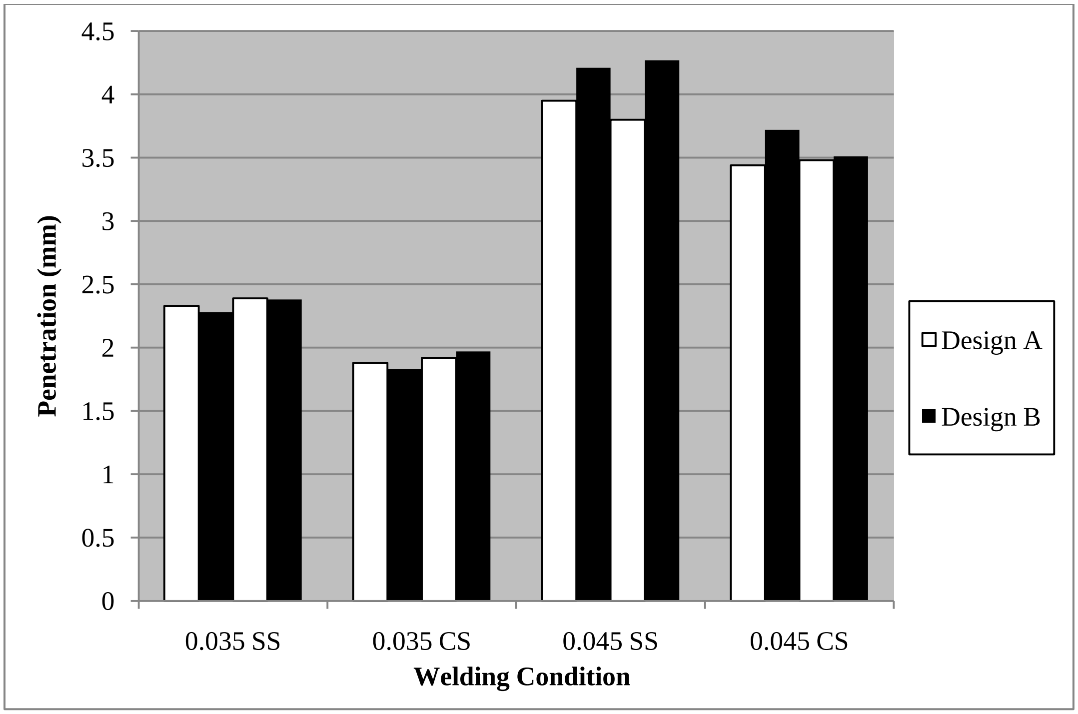

Figure 4-16
Penetration comparison between wire diameters and material type for each power supply design.

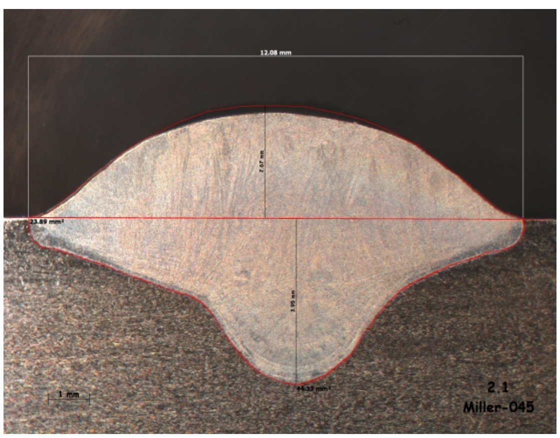

(a)

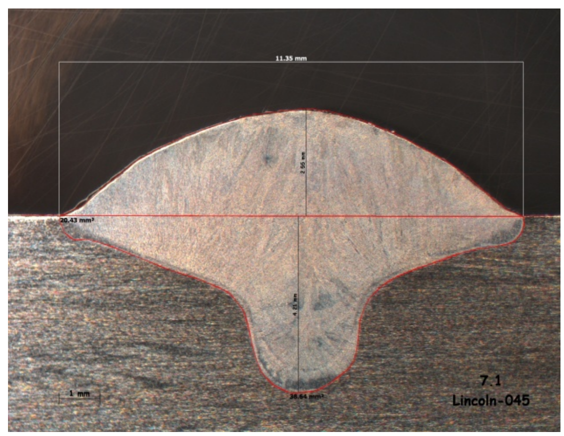

(b)

Figure 4-17
(a) Design A and (b) Design B with 0.045-in. stainless steel wire.

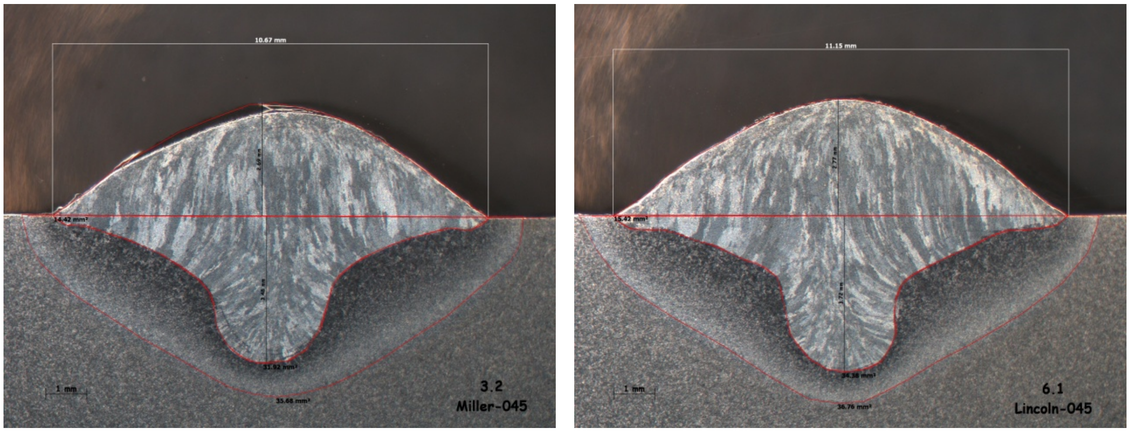

(a) (b)

Figure 4-18
(a) Design A and (b) Design B with 0.045-in. carbon steel wire.

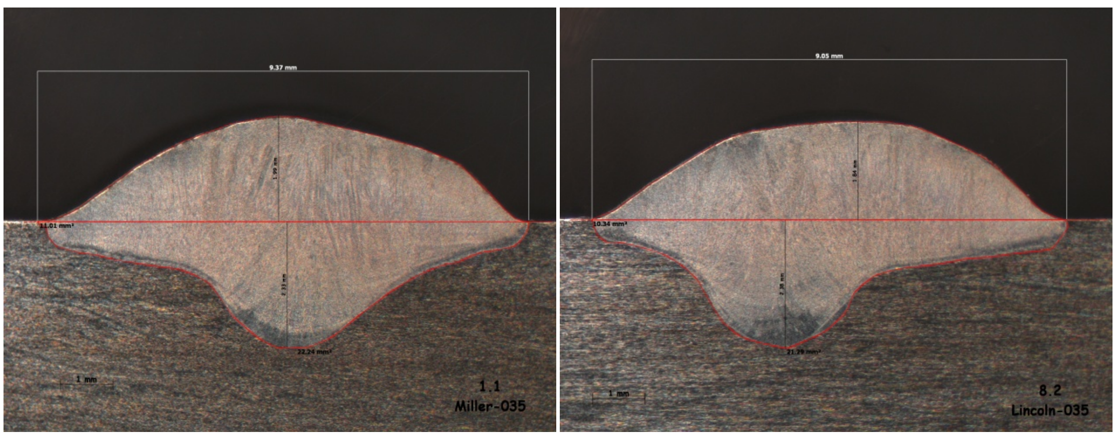

(a) (b)

Figure 4-19
(a) Design A and (b) Design B with 0.035-in. stainless steel wire.

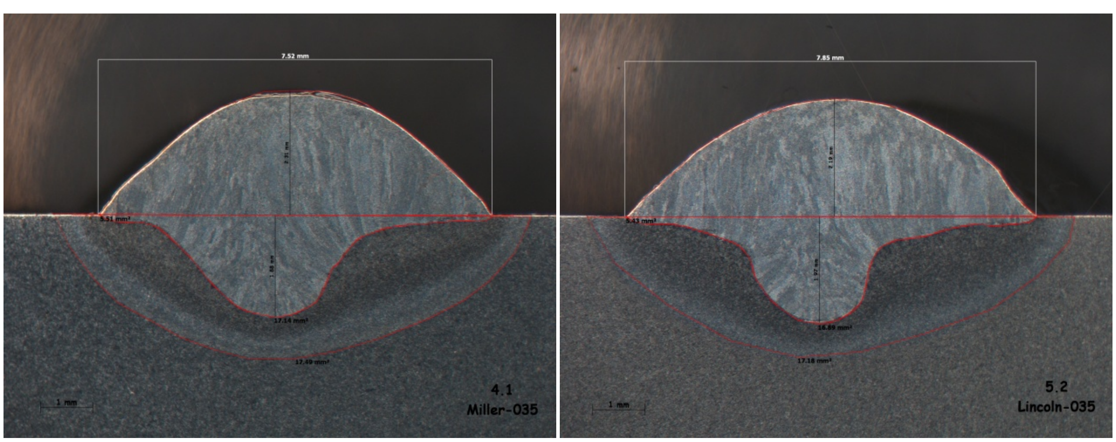

(a) (b)

Figure 4-20
(a) Design A and (b) Design B with 0.035-in. carbon steel wire.

5
CONCLUSIONS

1. All methods used to measure power produced similar reading and are viable options for the measurement of power; the maximum power difference between measurement methods was 3.45% for the same welding parameters.

2. Weld sizes were similar between welds made with different power sources and identical weld parameters.

3. Sampling rate is an important variable in power measurement and it must be sufficiently high to produce accurate readings.

6
REFERENCES

1. ASME Section IX QW409.1 and Appendix H, 2010: 69, 283-284
2. "Influence of GMAW-P current waveforms on heat input and weld bead shape", Farson, et al.
3. "Control of Penetration and Melting Ratio with Welding Technique", Jackson & Shrubsall
4. "The Effect of I2R Heating on Electrode Melting Rate", Jackson, Claussen, Wilson
5. "Influence of Weld Bead Area on Weld Metal Mechanical Properties", Shultz & Jackson
6. AWS Handbook, Volume 2, Eighth Edition
7. ASTM E340 Standard Test Method for Macro-etching Metals and Alloys
8. ASTM E3 Standard Guide for Preparation of Metallographic Specimens

Export Control Restrictions

Access to and use of EPRI Intellectual Property is granted with the specific understanding and requirement that responsibility for ensuring full compliance with all applicable U.S. and foreign export laws and regulations is being undertaken by you and your company. This includes an obligation to ensure that any individual receiving access hereunder who is not a U.S. citizen or permanent U.S. resident is permitted access under applicable U.S. and foreign export laws and regulations. In the event you are uncertain whether you or your company may lawfully obtain access to this EPRI Intellectual Property, you acknowledge that it is your obligation to consult with your company's legal counsel to determine whether this access is lawful. Although EPRI may make available on a case-by-case basis an informal assessment of the applicable U.S. export classification for specific EPRI Intellectual Property, you and your company acknowledge that this assessment is solely for informational purposes and not for reliance purposes. You and your company acknowledge that it is still the obligation of you and your company to make your own assessment of the applicable U.S. export classification and ensure compliance accordingly. You and your company understand and acknowledge your obligations to make a prompt report to EPRI and the appropriate authorities regarding any access to or use of EPRI Intellectual Property hereunder that may be in violation of applicable U.S. or foreign export laws or regulations.

The Electric Power Research Institute Inc., (EPRI, www.epri.com) conducts research and development relating to the generation, delivery and use of electricity for the benefit of the public. An independent, nonprofit organization, EPRI brings together its scientists and engineers as well as experts from academia and industry to help address challenges in electricity, including reliability, efficiency, health, safety and the environment. EPRI also provides technology, policy and economic analyses to drive long-range research and development planning, and supports research in emerging technologies. EPRI's members represent more than 90 percent of the electricity generated and delivered in the United States, and international participation extends to 40 countries. EPRI's principal offices and laboratories are located in Palo Alto, Calif.; Charlotte, N.C.; Knoxville, Tenn.; and Lenox, Mass.

Together…Shaping the Future of Electricity

1022881

Electric Power Research Institute
3420 Hillview Avenue, Palo Alto, California 94304-1338 • PO Box 10412, Palo Alto, California 94303-0813 • USA
800.313.3774 • 650.855.2121 • askepri@epri.com • www.epri.com